February 1, 2008

Vortex matter in mesoscopic superconductors

J. J. Palacios

Departamento de Física Teórica de la Materia Condensada

Universidad Autónoma de Madrid, Cantoblanco, Madrid 28049, Spain.

Abstract

Superconducting mesoscopic devices in magnetic fields present novel properties which can only be accounted for by both the quantum confinement of the Cooper pairs and by the interaction between the magnetic-field-induced vortices. Sub-micrometer disks, much the same as their semiconductor counterparts known as quantum dots, are being subject to experimental investigation by measuring their conducting properties and, more recently, their magnetization by using state-of-the-art ballistic Hall magnetometry. In this work I review the main results obtained in these two types of experiments as well as the current theoretical developments which are contributing to our understanding of the superconducting condensate in these systems.

Keywords: Superconductivity, vortices, mesoscopics.

Correspondence: Juan José Palacios

Address: Departamento de Física Teórica de la Materia Condensada,

Universidad Autónoma de Madrid, Cantoblanco, Madrid 28049, Spain

Fax: 34 91 397 4950

E-mail: palacios@kim.fmc.uam.es

I. INTRODUCTION

The physics of mesoscopic systems has reached its maturity within the semiconductor community over the past few years [1]. A similar revolution is nowadays taking place in superconductivity where superconducting device miniaturization is moving forward at a fast pace [2]. In both communities the concept of mesoscopics is directly linked to that of low-dimensionality. A system is called low-dimensional when at least one of the dimensions in which its carriers live becomes comparable to some relevant length scale intrinsically associated to bulk properties of those carriers. In semiconductors the most relevant length scale one can think of is the Fermi wavelength λ_F. In superconductors there are two fundamental length scales. One is the penetration length λ over which an externally applied magnetic field H is screened into the superconducting condensate. The other one is the coherence length ξ which, in a simple-minded picture, can be thought of as the size of the Cooper pairs and which limits the distance over which the superconducting order parameter can vary appreciably. When one of the dimensions of a semiconductor becomes comparable to λ_F, the other two being much larger, a two-dimensional electron gas (2DEG) is formed [1]. Similarly, typical superconducting thin films [2] can have a width comparable to either λ or ξ, or to both of them. If, in semiconductors, two out of the three dimensions become comparable to λ_F one forms a quantum wire [1]. A thin strip [3] can be thought of as the superconducting counterpart. When the three dimensions become comparable to either λ_F in semiconductors and to λ and/or ξ in supercondutors one speaks of 'zero-dimensional' systems called quantum dots [4–6] and thin disks [7–9], respectively. When the dimensions of the superconducting device become much smaller than ξ (as can be the case in very small metallic grains) the very notion of superconductivity needs to be revised [10]. The above classification, far from being unique and rigorous, only pretends to serve as a guide for the non-specialized reader.

It has been known for a long time that, in addition to the well-understood type-I superconductors where $\kappa = \lambda/\xi < 1/\sqrt{2}$, superconductors with $\kappa > 1/\sqrt{2}$ are also possible

(high-T_c materials are the most exotic example of them [2]). This seemingly inocent relation between the two fundamental lengths gives rise to type-II superconductivity which is characterized by the appearance of vortices in the superconducting condensate at values of H lying between a lower critical field H_{c1} and an upper critical field H_{c2}. An isolated vortex extends over a distance of the order of λ and exhibits a normal core of radius of the order of ξ [2]. A macroscopic number of vortices generically form a triangular lattice [11] which presents two well-characterized regimes or states: (i) a dilute vortex state (dVS) at low fields in which λ governs the inter-vortex distance and (ii) a dense vortex state (DVS) at high fields in which the fundamental length scale is given by ξ since the vortices are closely packed and their cores overlap strongly. In extreme type-II superconductors, characterized by $\kappa \gg 1$, the crossover from the dVS to the DVS takes place at rather low fields $H \approx 0.3 H_{c2}$ [12] which gives an idea of the relative importance of both regimes.

The dVS has been thoroughly studied over the years in all possible low-dimensional systems, both theoretical and experimentally. Many experimental techniques are sensitive to the vortex lattice in this regime, mainly due to the strong spatial modulation of the associated magnetic induction [12]. On the theory part, vortices in the dVS can be treated as classical, logarithmically-interacting, point-like particles which renders the calculation of the vortex structure free energy rather feasible in many different geometries [13–15]. By contrast, the structure of the DVS in nanostructures is difficult to unveil, partially due to the 'invisibility' of this state to the usual experimental techniques and to the difficulty in minimizing the free energy associated to this highly compacted vortex state when interfaces are present. Motivated by very recent advances in transport [7] and magnetometry techniques [8], which we review in Sec. II, we focus in this work on the theoretical study of the structural and magnetic properties of the DVS in superconducting thin disks or quantum dots. In Sec. III we show how to do this within the traditional framework of the Ginzburg-Landau functional in a rather analytical fashion. Finally, in Sec. IV we present our conclusions.

II. TWO RELEVANT EXPERIMENTS IN SUPERCONDUCTING MESOSCOPIC DISKS

One the most remarkable achievements in low-dimensional semiconductor physics has been the fabrication of the quantum dot or single-electron transistor where the electrons travel through the system one at a time and where the number of them present in the device can be tuned at will even down to a single electron [4,5]. These systems have been also given the name of artificial atoms since their generic properties are determined by both the quantum confinement and the interaction among the electrons much the same as in real atoms. Many analogies can be drawn between these artificial atoms and superconducting mesoscopic disks in perpendicular magnetic fields. Cooper pairs in disks can also experience the effects of quantum confinement and this becomes visible in the superconducting-normal phase boundary [7]. As far as the interaction is concerned the role of the electron is now played to some extent, not by the Cooper pair, but by another fundamental entity: The vortex. When the dimensions of the disk are comparable to λ in the dVS or to ξ in the DVS only few vortices can coexist in the disk. In contrast to the usual triangular arrangement in bulk, complex and unique vortex structures are expected to occur due to the competition between the geometrical confinement and the vortex-vortex interaction.

Transport experiments contributed in a decisive way to unveil the electronic structure of artificial atoms [5]. Similarly, conductance measurements [7] in individual mesoscopic disks gave us the first experimental evidence of the structure of the order parameter in these systems. Based on the onset of the disk resistance, oscillations of the critical temperature T_c as a function of the external magnetic field were measured and correctly accounted for by the quantization of the angular momentum L of the Cooper pair wavefunction. In more traditional words, they were observing transitions between giant vortex states with a different number L of fluxoids. These oscillations were clearly reminiscent of those observed in the famous Little-Parks experiment [16].

Transport measurements are necessarily bound to give only information about the crit-

ical phase boundaries since they are based on measuring the resistance of the non-fully superconducting state of the disk. Hall magnetometry [8], on the other hand, is revealing itself as a powerful tool for obtaining information of the order parameter away from the supercondutor-normal phase boundary. Thin superconducting Al disks are placed on top of a series of typical Hall probes created in a 2DEG. In the ballistic regime the Hall resistance is directly proportional to the average value of the magnetic field through the junction which, in turn, is determined by the magnetic state of the disk lying right above the junction. Magnetization (M) curves for different disk sizes can thus be obtained to exhibit a variety of unexpected phase transitions. For very small disks a first-order transition at a critical H_c, which is what one expects for a type-I superconductor as Al, is absent. For larger sizes this transition appears, but, on increasing further the disk radius the familiar second-order phase transition for a type-II superconductor, namely, an steady decrease of the magnetization beyond a certain critical H_{c1}, becomes notorious. On top of this steady decrease, the magnetization exhibits many jumps corresponding to first-order transitions which present an irregular and decreasing height as a function of H. All this seems to indicate that the quantum confinement is also patent in this experiment and that the Al disks are behaving like type-II superconductors rather than type-I, possibly due to the expected enhancement of the effective magnetic penetration length in such a geometry.

In the next section we show how many of these unexpected features can be obtained and explained within the traditional, phenomenological Ginzburg-Landau theory.

III. GINZBURG-LANDAU FUNCTIONAL APPROACH TO THE DVS IN SUPERCONDUCTING MESOSCOPIC DISKS

The theoretical analysis of the peculiar supercondutor-normal phase boundary measured in Ref. [7] does not present any difficulty since it simply implies solving the linearized Ginzburg-Landau equations [7,17–20]. The theoretical efforts to calculate the properties of the superconducting condensate in a disk well into the superconducting phase have been

mostly restricted to the dVS [14,15]. As far as the DVS is concerned, recent work is being done in the direction of solving numerically the Ginzburg-Landau equations either under the simplifying assumption of an order parameter with a well-defined L [20,21] or without any symmetry restrictions [8,22,23]. For type-II disks, the assumption of an order parameter with axial symmetry (well-defined L) does not hold. More precisely, it is only expected to hold in the Meissner state, which is associated to an $L = 0$ order parameter, and above H_{c2} [24] where, close to the surface of the disk, the superconductivity can survive up to a higher critical field H_{c3} [7,17–19]. This surface superconductivity is referred to as a condensed state of vortices or giant vortex [20–23]. For $H_{c1} < H < H_{c2}$ it was argued [20] and recently shown in numerical simulations [8,23] that the order parameter can form complex structures of single-fluxoid vortices, i.e., a "budding" Abrikosov lattice. From our more analytic stand-point the appearance of these structures necessarily implies an order parameter without a well-defined angular momentum L. Recent work in which this condition is explicitly taken into account has been presented in Ref. [9] and also in Ref. [23]. Part of the results presented here have already appeared in Ref. [9].

We start from the traditional Ginzburg-Landau functional for the Gibbs free energy of the superconducting state

$$G_{\rm s} = G_{\rm n} + \int d\mathbf{r} \left[\alpha |\Psi(\mathbf{r})|^2 + \frac{\beta}{2} |\Psi(\mathbf{r})|^4 + \right.$$
$$\left. \frac{1}{2m^*} \Psi^*(\mathbf{r}) \left(-i\hbar\nabla - \frac{e^*}{c} \mathbf{A}(\mathbf{r}) \right)^2 \Psi(\mathbf{r}) + \frac{[h(\mathbf{r}) - H]^2}{8\pi} \right], \tag{1}$$

where G_n is the Gibbs free energy of the normal state and $[-i\hbar\nabla - e^*\mathbf{A}(\mathbf{r})/c]^2/2m^*$ is the kinetic energy operator for Cooper pairs of charge $e^* = 2e$ and mass $m^* = 2m$ in a vector potential $\mathbf{A}(\mathbf{r})$ which is associated with the magnetic induction $h(\mathbf{r})$. The parameters α and β have the usual meaning [2]. Before proceeding any further we must stress a not fully appreciated fact: Even for small values of κ (≈ 1), the magnetic induction is weakly varying in space down to fairly low fields ($H \approx 0.5 H_{c2}$) [12]. Thus, it is a very good approximation to consider a uniform magnetic induction [$h(\mathbf{r}) = B$] down to $H \approx 0.5 H_{c2}$ and to expand the order parameter in the lowest Landau level (LLL):

6

$$\Psi(\mathbf{r}) = \sum_{L=0}^{\infty} C_L \frac{1}{\ell\sqrt{2\pi}} e^{-iL\theta} \Phi_L(r). \tag{2}$$

In this expansion $C_L \equiv |C_L|e^{i\phi_L}$ are complex coefficients and $\frac{1}{\ell\sqrt{2\pi}}e^{-iL\theta}\Phi_L(r)$ are normalized eigenfunctions of the kinetic energy operator in Eq. (1) plus the boundary conditions of zero current through the surface of the disk [25]. (We only consider disk thicknesses smaller than the coherence length so that the order parameter can be taken constant in the direction of the field.) Strictly speaking, these eigenfunctions are not LLL eigenstates. However, their radial part $\Phi_L(r)$, which may be found numerically, is nodeless and coincides with the radial function of the symmetric LLL eigenfunctions for small L. Figure 1 shows the Cooper pair band structure, i.e., the corresponding eigenvalues ϵ_L at different values of the external field for a disk of radius $R = 8\xi$ and $\kappa = \infty$ (this implies $H = B$). The horizontal lines represent $-\alpha$ which can be thought of as the chemical potential for the Cooper pairs. The formation of the dispersionless LLL in the center of the disk as the magnetic length $\ell = \sqrt{e^*\hbar/cB}$ becomes smaller than R is clearly visible. The bending of the band close to the surface is a consequence of the boundary condition and allows the nucleation of surface superconductivity (or the formation of a giant vortex) even when the bulk remains in the normal state ($H > H_{c2}$).

The expansion (2) captures both the simplicity of the macrovortex (above H_{c2}) when only one C_L is expected to be different from zero and the full complexity of the order parameter (below H_{c2}) when several components or harmonics must participate. Direct substitution of such an expansion into Eq. 1 and subsequent numerical minimization of the resulting expression is a daunting task bound to fail due to the large number of unknown variables involved. Instead, it is preferable to consider expansions in restricted sets $\{L_1, L_2, \ldots, L_N\}$ of few N components where $L_1 < L_2 < \ldots < L_N$. The difference between the Gibbs free energies of the normal and superconducting phases takes the following form for each set:

$$G_{\text{s}} - G_{\text{n}} = \sum_{i=1}^{N} \alpha[1 - B\epsilon_{L_i}(B)]|C_{L_i}|^2 + \frac{1}{4}\alpha^2\kappa^2 BR^2 \times$$
$$\left[\sum_{i=1}^{N} I_{L_i}(B)|C_{L_i}|^4 + \sum_{j>i=1}^{N} 4I_{L_iL_j}(B)|C_{L_i}|^2|C_{L_j}|^2 + \right.$$

$$\sum_{k>j>i=1}^{N} 4\delta_{L_i+L_k,2L_j} \cos(\phi_{L_i} + \phi_{L_k} - 2\phi_{L_j})$$

$$I_{L_iL_jL_k}(B)|C_{L_i}||C_{L_j}|^2|C_{L_k}| +$$

$$\sum_{l>k>j>i=1}^{N} 8\delta_{L_i+L_l,L_j+L_k} \cos(\phi_{L_i} + \phi_{L_l} - \phi_{L_j} - \phi_{L_k})$$

$$I_{L_iL_jL_kL_l}(B)|C_{L_i}||C_{L_j}||C_{L_k}||C_{L_l}| \Big] + (B-H)^2, \tag{3}$$

where $G_{\mathrm{s}} - G_{\mathrm{n}}$ and α are given in units of $H_{\mathrm{c2}}^2 V/8\pi$ (V is the volume of the disk), $\epsilon_L(B)$ is given in units of the lowest Landau level energy $\hbar\omega_c/2$ (with $\omega_c = e^* B/m^* c$), R is in units of ξ, and B and H are given in units of H_{c2}. The terms proportional to α contain the condensation and kinetic energy of the Cooper pairs. All the other terms, which are proportional to α^2, account for the "interaction" between Cooper pairs. There appear four types of these terms: (i) those proportional to $I_L(B) \equiv \int dr \, r \, \Phi_L^4$, reflecting the interaction between Cooper pairs occupying the same quantum state L, (ii) those proportional to $I_{L_iL_j}(B) \equiv \int dr \, r \, \Phi_{L_i}^2 \Phi_{L_j}^2$, reflecting the interaction between Cooper pairs occupying different quantum states, and (iii) the ones proportional to $I_{L_iL_jL_k}(B) \equiv \int dr \, r \, \Phi_{L_i} \Phi_{L_j}^2 \Phi_{L_k}$ and proportional to $I_{L_iL_jL_kL_l}(B) \equiv \int dr \, r \, \Phi_{L_i} \Phi_{L_j} \Phi_{L_k} \Phi_{L_l}$ which, along with the phases ϕ_L, are responsible for the spatial correlation between vortices and the detailed structure of the DVS (see below). The non-linear dependence on B of these integrals [as well as that of $\epsilon_L(B)$] comes from the existence of the disk surface.

In order to find the minimum Gibbs free energy for a given set we have to minimize with respect to the moduli $|C_{L_1}|, \ldots, |C_{L_N}|$, the phases $\phi_{L_1}, \ldots, \phi_{L_N}$ of the coefficients, and with respect to B. The minimum-energy set of components is picked up at the end. The advantage of doing this selective minimization resides in our expectation that a small number of components will suffice to describe the order parameter for disks with radii of few coherent lengths. As illustrative and relevant examples we consider in the detail the solutions with one and two components. For $N = 1$ the energy functional is invariant with respect to the phase of the only coefficient so one can minimize analytically with respect to $|C_L|^2$ to obtain

$$G_{\mathrm{s}} - G_{\mathrm{n}} = -\frac{[1 - B\epsilon_L]^2}{\kappa^2 B R^2 I_L} + (B-H)^2, \tag{4}$$

8

where we have dropped the implicit B-dependences. Finally, the minimal value of B and the minimum Gibbs free energy for each L must be found numerically. The 2-component solutions $\{L_1, L_2\}$ can be dealt with in a similar way. The energy functional is invariant with respect to the phases so one can minimize analytically with respect to $|C_{L_1}|^2$ and $|C_{L_2}|^2$ to obtain

$$G_s - G_n = -\frac{[1 - B\epsilon_{L_1}]^2 I_{L_2} + [1 - B\epsilon_{L_2}]^2 I_{L_1} - 4[1 - B\epsilon_{L_1}][1 - B\epsilon_{L_2}]I_{L_1 L_2}}{\kappa^2 B R^2 [I_{L_1} I_{L_2} - 4 I_{L_1 L_2}]} + (B - H)^2 \quad (5)$$

and numerically with respect to B to obtain the minimum energy for the given pair of components. The superconducting condensate looks generically like an $(L_2 - L_1)$-vortex ring. It is important to notice that α disappears from the final expressions (4) and (5) which leaves us with κ as the only adjustable parameter when comparing with experiments. (This is also true for the more complex cases discussed below). For 3-component solutions (two vortex rings) the energy functional is still invariant with respect to all the three phases whenever $L_1 + L_3 \neq 2L_2$, and, once again, the minimization with respect to $|C_{L_1}|^2$, $|C_{L_2}|^2$, and $|C_{L_3}|^2$ can be done analytically. However, if $L_1 + L_3 = 2L_2$, the two rings have the same number of vortices and their relative angular positions come into play through the term depending on the phases. There is, however, an obvious choice for these phases: $\phi_{L_1} = 0, \phi_{L_2} = 0, \phi_{L_3} = \pi$. This choice gives a negative contribution to the free energy which reflects a lock-in position between the vortex rings. In general, the minimum-energy solutions for disks are expected to have strongly overlapping components which invalidates any perturbative treatment of the terms that contain the phases [3]. Moreover, unlike simpler geometries [3], there is no direct connection between number of components in which we expand the order parameter and number of vortices. This prompts us to seek solutions through numerical minimization with respect to the moduli and B for the 3-component cases just mentioned, and, for $N > 3$, with respect to the moduli, the phases, and B whenever the terms involving phases are present. For the disk sizes like the ones used in the experiment of Ref. [8] 2 and 3-component solutions suffice to capture the relevant physics.

Figure 2 shows the magnetization as a function of H for two disks with $\kappa = 2$. The com-

ponents or harmonics with significant weight corresponding to the minimum-energy order parameter at each magnetization step are also shown. For the smaller disk of radius $R = 4\xi$ we obtain a series of first-order transitions. Here all the minimal solutions correspond to giant vortices which contain L fluxoids. Whenever L changes by one the magnetization presents a (non-quantized) jump whose magnitude evolves *monotonously* with L. For the larger $R = 7\xi$ disk $N > 1$ solutions appear below H_{c2}. In this case, allowing more components in the expansion of the order parameter has a fundamental effect: It splits the giant vortex into a complex vortex glass structure of many single-fluxoid vortices [see Figs. 3(a) to (c)]. This glass structure reflects in the magnetization curves by changing the regular evolution of the magnitude of the jumps into an irregular one. Whenever a vortex is added or removed from the disk the symmetry of the new vortex configuration changes which, in turn, expels the field in a different way. The total number of vortices is always given by the largest L_N which does not depend on the value of L of the other harmonics: Only the internal arrangement of vortices does. There usually exist configuration switches for a given number of vortices (i.e., for a given L_N), but these changes *do not* reflect in the magnetization (see Fig 2). On top of the first-order transitions the overall slope in the magnetization clearly changes at H_{c2}, i.e., at the transition between the giant vortex and the vortex glass structures. This transition is reminiscent of the second-order transition at H_{c2} for bulk samples where M vanishes.

Finally, we point out that the magnetization measured by Geim et al. in Ref. [8] presents features that are in good agreement with our results despite of the fact that the disks are made out of a strong type-I material as Al. It is well known that the bulk value of κ can increase in the plate geometry [26]. To compare with the experiment, we simulate this fact by using a higher value of κ than the nominal one. In Fig. 4 we show the data for a disk of nominal radius $R = 5\xi$ and thickness $d = 0.6\xi$. We have obtained a reasonable good agreement in the number and magnitude of the jumps, and overall shape of the magnetization using $R \approx 5\xi$ and $\kappa \approx 1$ (the dotted line is a good example). This is consistent with an effective penetration length longer than expected and, possibly, with a coherence length

shorter than the bulk nominal one. Although, due to the smallness of the disk, it is difficult to point at a second-order phase transition, the non-monotonous evolution of the magnitude of the magnetization jumps is notorious over a large range of fields which, as we have shown, is an indication of the formation of vortex glass structures. In our approximation the magnetic induction is uniform in space, but, given the good agreement with the experimental curve, this does not seem to be an important restriction.

IV. CONCLUSIONS

After reviewing some of the state-of-the-art experiments in mesoscopic superconductivity we have shown how to calculate the dense vortex matter structure and associated magnetization for type-II superconducting mesoscopic disks. We have found that the magnetization exhibits generically a first-order phase transition whenever the number of vortices changes by one with H. It also presents two well-defined regimes: A *non-monotonous* evolution of the magnitude of the jumps signals the presence of a vortex glass structure which is separated by a second-order phase transition at H_{c2} from a condensed state of vortices (giant vortex) where the magnitude of the jumps changes monotonously. We have compared our results with the Hall magnetometry measurements in Ref. [8] and claimed that the magnetization exhibits clear traces of the presence of these vortex glass states.

V. ACKNOWLEDGEMENTS

REFERENCES

[1] See for instance Physica E 1 (1997).

[2] For a review on classical and modern topics in superconductivity see for instance M. Tinkham, *Introduction to Superconductivity*, 2nd Ed. (McGraw-Hill, New York, 1996).

[3] J. J. Palacios, Phys. Rev. B 57 (1998) 10873.

[4] R. C. Ashoori, Nature 379 (1996) 413.

[5] L. Kouwenhoven *et al.*, Science 278 (1997) 1788.

[6] J. J. Palacios, L. Martín-Moreno, G. Chiappe, E. Louis, and C. Tejedor, Phys. Rev. B 50 (1994) 5760.

[7] V. V. Moshchalkov *et al.*, Nature 373 (1995) 319.

[8] A. K. Geim *et al.*, Nature 390 (1997) 259.

[9] J. J. Palacios, Phys. Rev. B 58 (1998), R5948. cond-mat/9806056.

[10] F. Braun, Jan von Delft, D. C. Ralph, and M. Tinkham, Phys. Rev. Lett. 79 (1997) 921.

[11] A. A. Abrikosov, Zh. Eksp. Teor. Fiz. 32 (1957) 1442 [Soviet Phys. JETP 5 (1957) 1174].

[12] For a recent example of an accurate calculation of bulk vortex lattices at any value of the magnetic induction see E. H. Brandt, Phys. Rev. Lett. 78 (1997) 2208.

[13] J. Guimpel et al., Phys. Rev. B 38 (1988) 2342; S. H. Brongersma et al. Phys. Rev. Lett. 71 (1993) 2319; M. Ziese et al. Phys. Rev. B 53 (1996) 8658; F. F. Ternovskii and L. N. Shekhata, Zh. Eksp. Teor. Fiz. 62 (1972) 2297 [Soviet Phys. JETP 35 (1972) 1202].

[14] A. I. Buzdin and J. P. Brison, Phys. Lett. A 196 (1994) 267.

[15] P. A. Venegas and E. Sardella (unpublished), cond-mat/9804144.

[16] W. A. Little and R. D. Parks, Phys. Rev. Lett. 9 (1962) 9.

[17] R. Benoist and W. Zwerger, Z. Phys. B 103 (1997) 377.

[18] A. I. Buzdin, Phys. Rev. B 47 (1993) 11416.

[19] A. Bezryadin, Y. N. Ovchinnikov, and B. Pannetier, Phys. Rev. B 53 (1996) 8553.

[20] V. V. Moshchalkov, X. G. Qiu, and V. Bruyndoncx, Phys. Rev. B 55 (1997) 11 793.

[21] P. S. Deo, V. A. Schweigert, F. M. Peeters, and A. K. Geim, Phys. Rev. Lett. 79 (1997) 4653; V. A. Schweigert and F. M. Peeters, Phys. Rev. B 57 (1998) 13 817.

[22] P. S. Deo, V. A. Schweigert, F. M. Peeters (unpublished), cond-mat/9804174.

[23] V. A. Schweigert, P. S. Deo, F. M. Peeters, (unpublished), cond-mat/9806013.

[24] Notice that H_{c2} for a disk of an intrinsic type-II material is larger than that for the same material in bulk since the surface superconductivity carries a supercurrent and, consequently, a magnetization. For simplicity's sake we are not making any distinction here.

[25] P. G. deGennes and D. Saint-James, Phys. Lett. 7 (1963) 306; H. J. Fink, Phys. Rev. Lett. 14 (1965) 309.

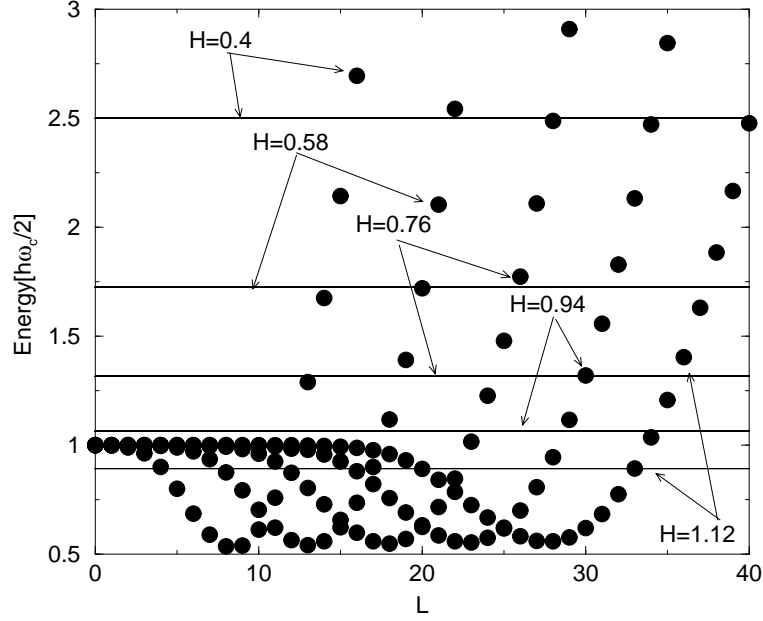[26] G. J. Dolan, J. Low Temp. Phys. 15 (1974) 111.

FIGURES

FIG. 1. Band structure and chemical potential $(-\alpha)$ of the Cooper pairs at different values of H (in units of H_{c2}) for a disk of radius $R = 8\xi$ and $\kappa = \infty$. Notice that, for fields above H_{c2}, the lowest Landau level can lie below the chemical potential only close to the surface of the disk. This gives rise to the formation of a giant vortex with an L around the bottom of the band.
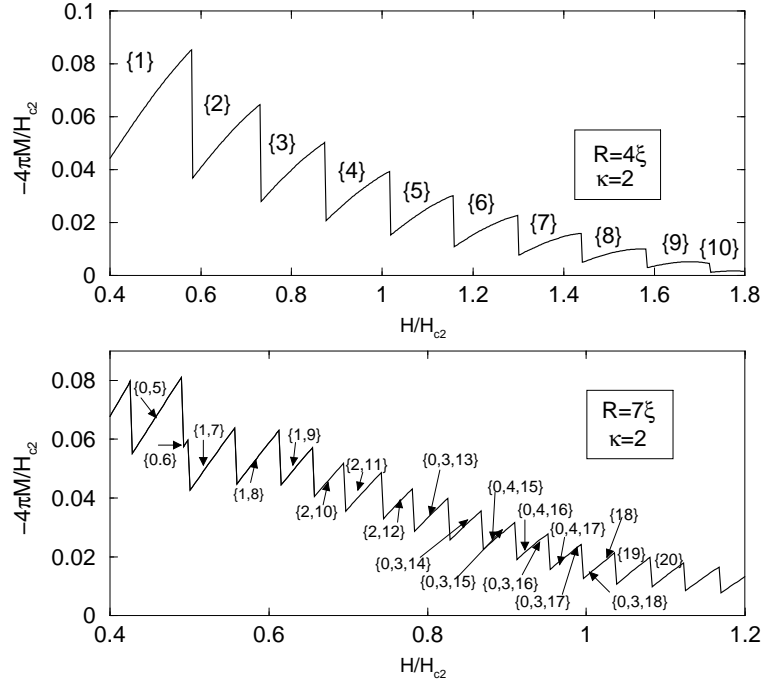
FIG. 2. Magnetization as a function of H for two disks of $\kappa = 2$ and radius (a) $R = 4\xi$ and (b) $R = 7\xi$. The sets of harmonics with significant weight corresponding to the expansion of the order parameter at each magnetization step are also shown.
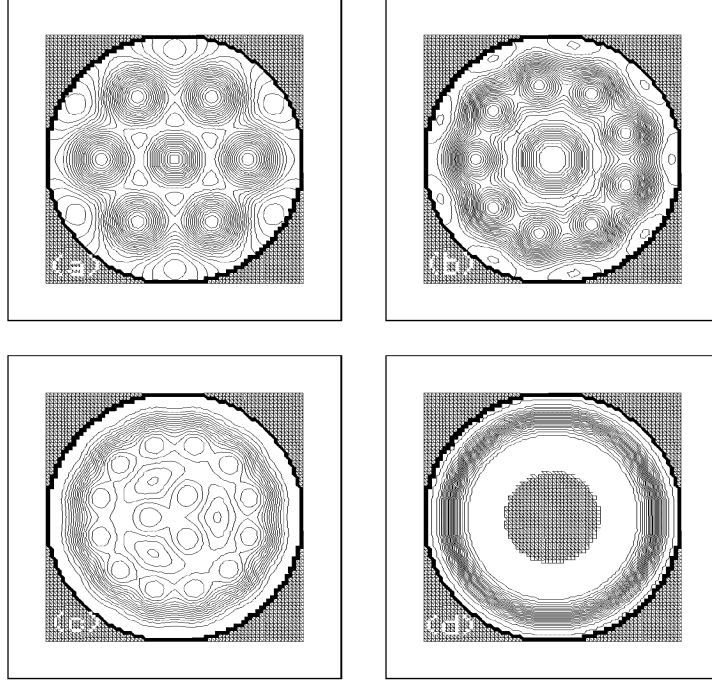

FIG. 3. Superconducting condensate in the DVS for an $R = 7\xi$, $\kappa = 2$ disk at (a) $H = 0.5H_{c2}$, (b) $H = 0.7H_{c2}$, (c) $H = 0.9H_{c2}$, and (d) $H = 1.1H_{c2}$. Below H_{c2} the density associated to the order parameter presents a vortex glass structure which disappears above H_{c2} into a condensate of vortices or giant vortex. Notice the appearance in (b) of two-fluxoid vortices even below H_{c2}.
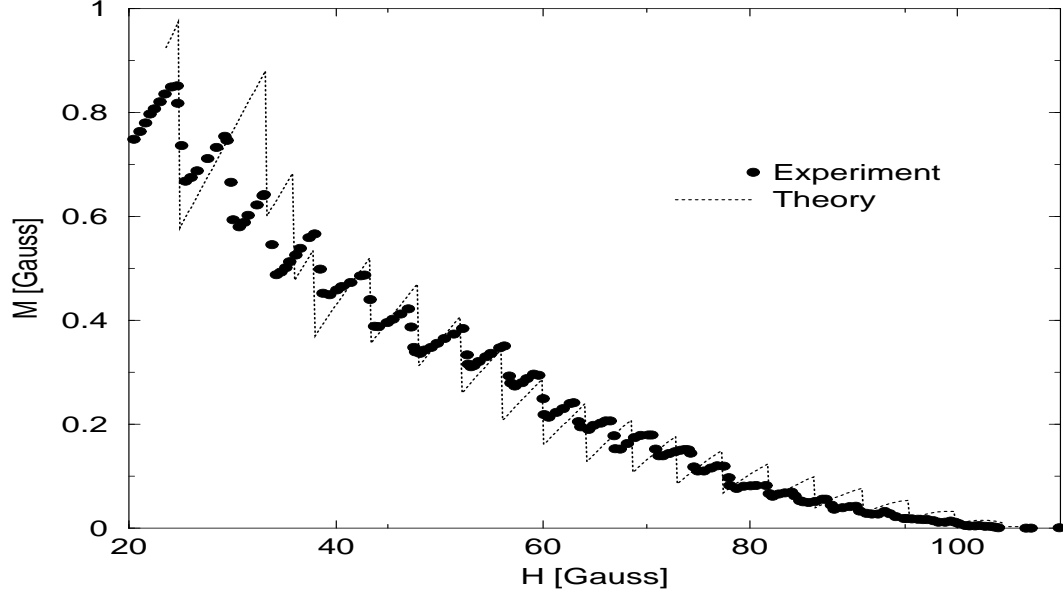
FIG. 4. Comparison between experimental data (reproduced from Refs. [21]) and theory using $R = 5.25\xi$ and $\kappa = 1.2$. Similar considerations as in Refs. [21] have been followed for the adjustment of the theoretical curve.